AN IN-DEPTH ANALYSIS AND IMAGE QUALITY ASSESSMENT OF AN EXPONENT-BASED TONE MAPPING ALGORITHM

Chika Ofili, Stanislav Glozman, Orly Yadid-Pecht

Abstract: *In order to view wide contrast details in an image scene, a wide dynamic range (WDR) image sensor is required. However, these wide dynamic range images cannot be accurately viewed on a regular display device due to its limited dynamic range. Without the proper use of a WDR image compression algorithm, the details of images will be lost. Tone-mapping algorithms are used to adapt the captured wide dynamic range scenes to the low dynamic range displays available. This paper explores the utilization of an exponent-tone mapping algorithm for colored and monochrome WDR images in lure of a regular display. The exponent-based tone mapping algorithm utilizes only the Bayer (CFA) of the WDR image to produce tone mapped image results. High quality results are achieved without the use of additional image processing techniques such as histogram clipping. The image results are then compared with other conventional tone mapping operators available.*

Keywords: *Tone mapping, Wide dynamic range, High Dynamic Range Image, Image enhancement.*

ACM Classification Keywords: *A.0 General Literature - Conference proceedings; I.4.0 Image processing and Computer Vision- General (or .3 enhancement)*

Introduction

A. Wide dynamic range Imaging:

In imaging, dynamic range can be described as the luminance ratio between brightest and darkest parts of a scene [1]. Natural sceneries have a wide dynamic range that is of five-six orders of magnitude, while commonly used display devices have a limited dynamic range. The dynamic range of most available display devices is of two orders of magnitude, which represent 2^8 (256) levels of radiance [2].

Emerging image capture devices can produce wide dynamic range images which have higher dynamic range in comparison to available limited range display devices [3]. However, when these captured wide dynamic range images are being displayed on these commonly used devices, they appear to be over-exposed in well-lit scenes or under-exposed in dark scenes (Figure 1). Hence, image details will be lost when displayed.

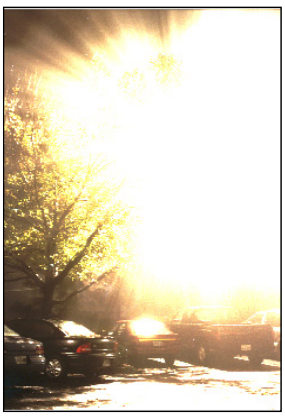

Figure 1: Under-exposed Image (left), Overexposed Image (right)

In order for the images to be accurately represented, tone-mapping algorithm is used to adapt the captured wide dynamic range scenes to the low dynamic range displays available (Figure 2).

Figure 2: Under exposed WDR image (left) and
enhanced image using Glozman et al [4] tone mapping algorithm (right)

B. Tone mapping Algorithms

There are two main categories of tone-mapping algorithms; Tone Reproduction curves (TRC) and Tone Reproduction Operators (TRO) [2].

TRC (also known as global tone mapping operator) maps all the image pixel values to a display value without taking into consideration the spatial location of the pixel in question [2]. Hence, one input pixel value corresponds to only one output pixel value. The mapping function can be a gamma, a power function, a logarithmic or a function with adaptation to the image key [5].

Conversely, TRO (also called local mapping operator) is spatial location dependent and varying transformations are applied to each pixel depending on its surrounding [2]. Hence, one input pixel value may result in different output values.

There has been a lot of progress in the development of global and local tone mapping algorithms respectively [2] [5-11]. Most tone mapping operators perform only one type of tone mapping operation (global or local). However, Meylan et al, Kats et al, Glozman et al and Shin et al [4, 5, 7, 12] have developed tone-mapping algorithms that contain both local and global mapping operators.

There are trade-offs that exist in relation to which method of tone mapping is being use used. TRC algorithms are generally less time consuming and require less computational effort but can result in loss of local contrast due to the global compression of the dynamic range [3]. In general, TRO algorithms do not result in loss of local contrast, but they require more computational effort and may result in the addition of image artifacts such as halos [4]. Consequently, TROs are less suitable for hardware implementation in comparison to TRC based algorithms.

The tone mapping algorithm developed by Glozman et al [4] achieved the goal of compressing wide range of pixel values into a smaller range that is suitable for display devices with less heavy computational effort. The simplicity of this tone mapping operator makes it a suitable algorithm that can be used as part of a system-on-chip. In this paper, an in-depth analysis of the algorithm, as well as how various modifications applied to the algorithm affects its performance will be explored. In addition, the comparison of the algorithm with other tone mapping operators in terms of computational time and image quality will be examined.

C. Exponent-based Tone mapping Operator

The algorithm implementation follows the approach proposed by Meylan et al [5] which implements the tone-mapping algorithm directly on the color filter array (CFA) data (Figure 3). This approach is different from other

traditional processing workflows that implemented rendering operations after demosaicing the CFA image. This reduces the complexity of the tone mapping algorithm needed for a colored image because the algorithm is applied to only 1/3rd of the image.

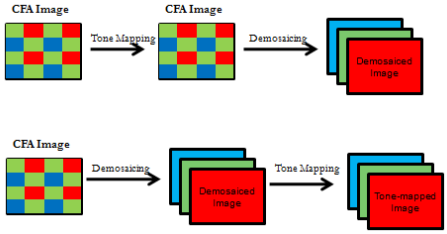

Figure 3: (Top) Approach developed by Meylan et al [5]
and traditional image processing workflow (bottom)

In the tone mapping algorithm proposed by Glozman et al [4] an inverse exponent function (1) is applied directly on the CFA.

$$Y(p) = 1 - e^{-\frac{X(p)}{X_o(p)}} \quad (1)$$

Where p is a pixel in the image, X(p) represents specific CFA pixel's input light intensity, Y(p) is the pixel's adapted signal and $X_o(p)$ is the adaptation factor of the specific CFA pixel (2). $X_o(p)$ varies for each pixel p and comprises of both a global and a local component.

$$X_o(p) = K.X_{DC} + X(P) * G_H \quad (2)$$

Where X_{DC} is the mean value of all the CFA image pixel intensities; K is the image coefficient that varies from [0 1]; "$*$" denotes the convolution operation; and G_H is a two-dimensional Low pass filter that models dependency of the $X_o(p)$ on the light intensity of the surrounding pixels.

A scaling coefficient (3) is added to equation 1 so as to ensure that all the tone mapping curves will start at the origin and meet at $X(p)=X_{max}$.

$$Y(p) = \frac{X_{max}}{\left(1 - e^{-\frac{X_{max}}{X_o(p)}}\right)} . \left(1 - e^{-\frac{X(p)}{X_o(p)}}\right) \quad (3)$$

The effects of the tone mapping parameters i.e. factor, K and the low pass filter will be discussed in the next section.

Effects of Tone mapping Parameters

K Factor

As stated above, the adaptation factor $X_o(p)$ in equation 2 consist of a global and local image processing. The global component in $X_o(p)$ comprises of factor K, and the global mean of the image X_{DC}. The amount global tonal correction done is modulated by factor K. The factor K can be adjusted between 0 and 1 depending on the image key. Low and high key images are images that have a mean intensity that is lower or higher than average [13]. K factor values closer to 0 are needed for low key images while values closer to 1 are needed for high key images. This is because the lower the K value, the higher the image contrast and overall image luminance. While

the higher the K value, the higher the compression of higher pixel values and the overall image appears less exposed (Figure 4 & 5).

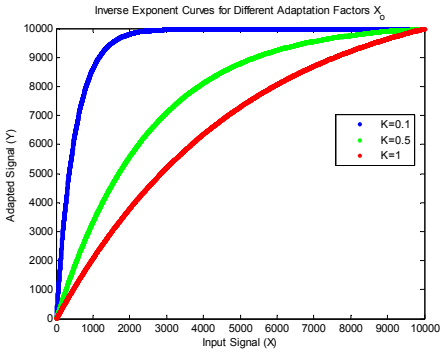

Figure 4: Inverse exponent curves for different K values

Figure 5: Memorial image (from the Devebec Library) with same low pass filter size. A. K=1, B. K=0.5 C. K=0.25 D. K=0.125

Figure 6: Dani_Cathedral image [14] with same low pass filter size. A. K=1, B. K=0.5 C. K=0.25 D.

Local Image processing: Filter

The second component in the adaptation equation (2) is the local image computation. To obtain the local component, information of the neighboring pixels is acquired. This is done by using an image filter. Various local

tone mapping operators utilize different image filters such as low pass filters, edge-preserving low pass filters, and or multi-scale pyramids to obtain the spatial localized content [14].

With tone mapping operators that involve local processing, artifacts such as halos could occur. This is because the pixels in close proximity to a specified pixel could have a very different light intensity that could result in contrast reversals [15]. Different image filters are described below and the benefits and drawbacks are examined. The aim is to find a filter that will result in less halo artifacts.

Gaussian filter:

This is a simple low pass filter that takes an average of the neighboring pixels. The average is taken in such a way that the pixels nearest to the centre pixel contribute more to the result than those further away [16]. Because it also takes into consideration the pixel values that represent edges in an image, artifacts such as halos may appear along those edges (Figure 7-8). The occurrence of contrast reversal depends on the size of the filter [11]. The kernel size in Figure 8 is smaller than the one used in Figure 7 and it has less presence of halos but also image contrast has reduced.

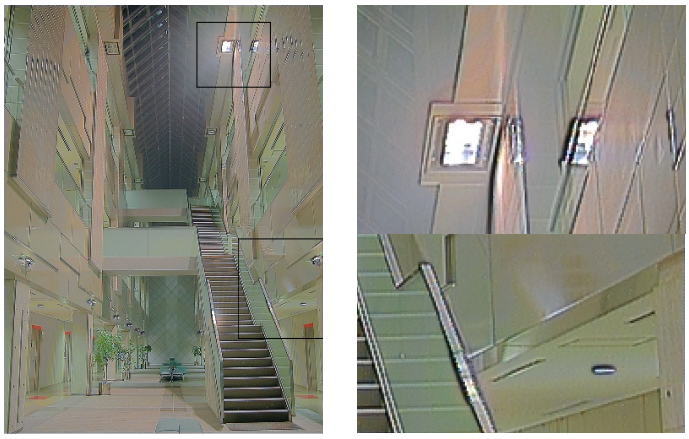

Figure 7: Tone mapped WDR image using a Gaussian filter (Kernel size=8, σ=1)

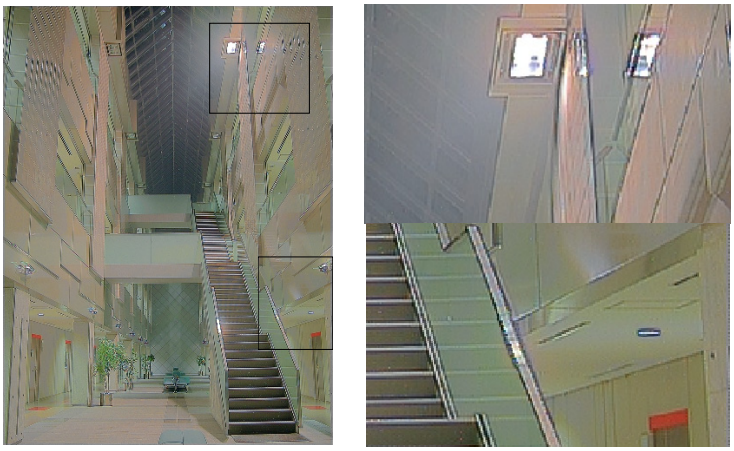

Figure 8: Tone mapped WDR image [17] using a Gaussian filter (Kernel size=3, σ=1)

Median filter:

In a median filter, the output intensity of a given pixel is the median intensity value of the pixels within a given odd sized window [18]. Based on the filter window size, it sorts the pixel values in ascending order and the median pixel value in the sorted array is stored. This makes ~~is~~ a good edge preserving filter because extremely high and low values are avoided thereby, reducing the occurrence of halos artifacts (Figure 9). Although, a key disadvantage of median filters is the loss of fine details and also presence of unexpected artifacts (Figure 10); this setback can be eliminated by reducing the size of the kernel being used (Figure 11).

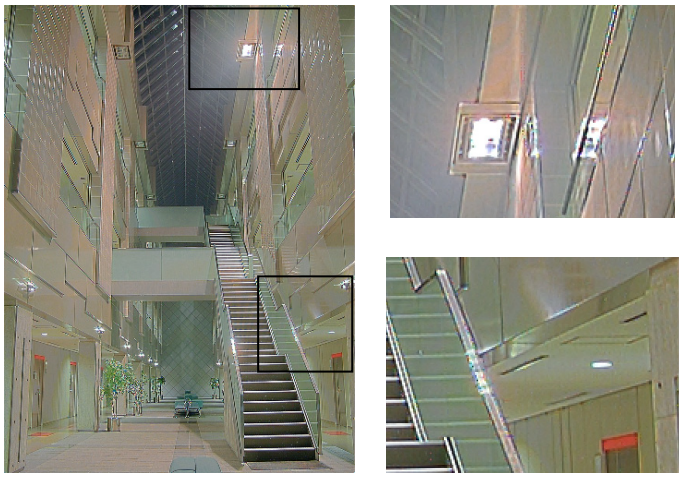

Figure 9: Tone mapped WDR image [17] using a Median filter (Kernel =7)

Figure 10: Tone mapped WDR image [19] using a Median filter (Kernel =7).

Figure 11 : Tone mapped WDR image [19] using a Median filter (Kernel =3).

Anisotropic Gaussian Filter:

This is a Gaussian-inspired filter that preserves the contrast at the edges unlike a simple Gaussian filter. It is based on the heat diffusion equation; it is modified to preserve edges by reducing the heat dissipated at the edges and at the same time, smoothen similar image [20].

It helps reduce the presence of halos and also increased the contrast as shown in Figure 12. However, it will be harder to implement on hardware in comparison to a Gaussian filter.

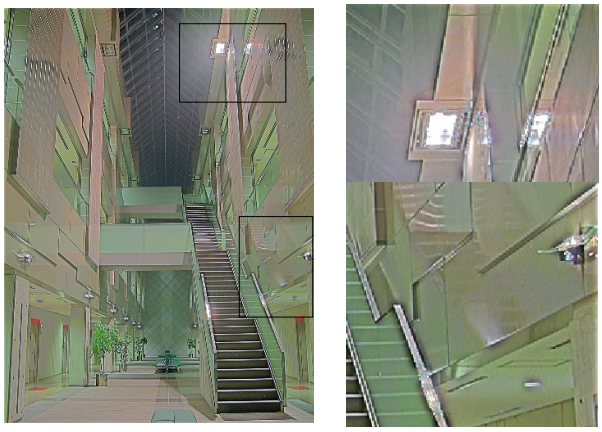

Figure 12: Tone mapped WDR Image [17] using an Anisotropic Gaussian filter.

Sigma Filter:

A sigma filter is a modified mean filter that also preserves edges. Each output pixel is an average of the surrounding input pixels that lie within an intensity range in relation to the central pixel [21]. The intensity range is described as 2*σ, where σ is an integer value. Using equation 4,

$$Y(p) = \frac{\sum_K \delta . X}{\sum_K \delta} \tag{4}$$

Where Xp is light intensity of pixels in the specified window size K, δ is used to determine which neighbouring pixels are included in the calculation of the mean. The matrix δ is obtained using equation 5

$$\delta_{i,j} = \begin{cases} 1, & \text{if } \left|X_{i,j} - X_{\text{centre pixel}}\right| \leq 2\sigma \\ 0, & \text{if } \left|X_{i,j} - X_{\text{centre pixel}}\right| > 2\sigma \end{cases} \tag{5}$$

To prevent having too few pixels involved in the calculation, the mean of the pixels within the window is used instead when the number of pixels that are within the specified intensity range is less than a specified number N [21]. Simulations done showed that decreasing the value of σ and N will reduce presence of halos.

In the results shown (Figure 13), the sigma σ, was set at 2, while the kernel size was 5. The filter preformed better in reducing the presences of halos (unlike the Gaussian filter) and did not result in unusual artefacts like the median filter. It will also be relatively easy to implement on hardware.

Figure 13: Tone mapped WDR Image [17] using a 5x5 Sigma filter (N=12 and σ=2).

Bilateral Filter:

Bilateral filtering is a non-linear filter in which each output is a weighted average of the surrounding input pixels. Unlike the Gaussian filter, it also acts as an edge preserving filter. This is because the weight is determined from the proximity of the pixels to the pixel in question and the intensity difference between the neighboring pixels and the current pixel [22]. The weighting of the pixels deceases as the intensity difference increases [23]. Hence, this will help reduce the possibility of halo artifacts.

There is still some presence of halo artifacts but it produces a better output in comparison to the Gaussian filter (Figure 14). However, this method will not be power efficient for hardware implementation.

Figure 14: Tone mapped WDR image [17] using bilateral filter.

From simulation done on several images [11, 19], the exponent based tone mapping [4] with a sigma filter for local adaptation, was found to be the best (Figure 15-17). This is because, it had less halos, in comparison to the Gaussian filter, and it will require less computation in comparison to the anisotropic Gaussian filter and the bilateral filter. In some cases, the image produced by the anisotropic Gaussian filter had too much contrast (Figure 16). In addition, the sigma filter will correlate better with the way the eyes performs local adaptation (in comparison to the median filter). The median filter produced the best results in most cases, except in cases like Figure 10.

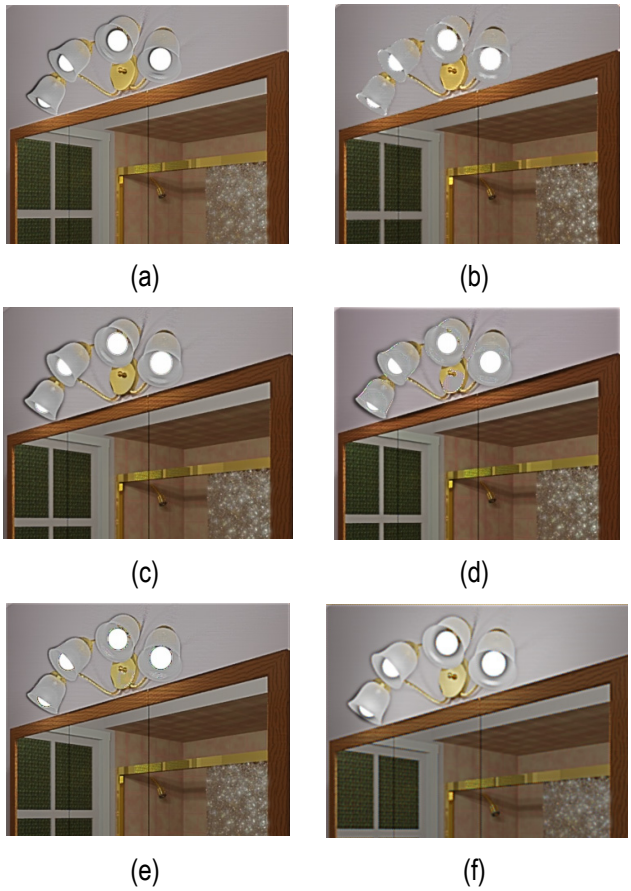

(a) (b)

(c) (d)

(e) (f)

Figure 15: Tone mapped WDR image [24] using a. Gaussian filter (7x7), b. Median Filter (7x7), c. Bilateral Filter, d. Anisotropic Gaussian filter (7x7), e. Sigma Filter (7x7), f. S. Meylan method [5].

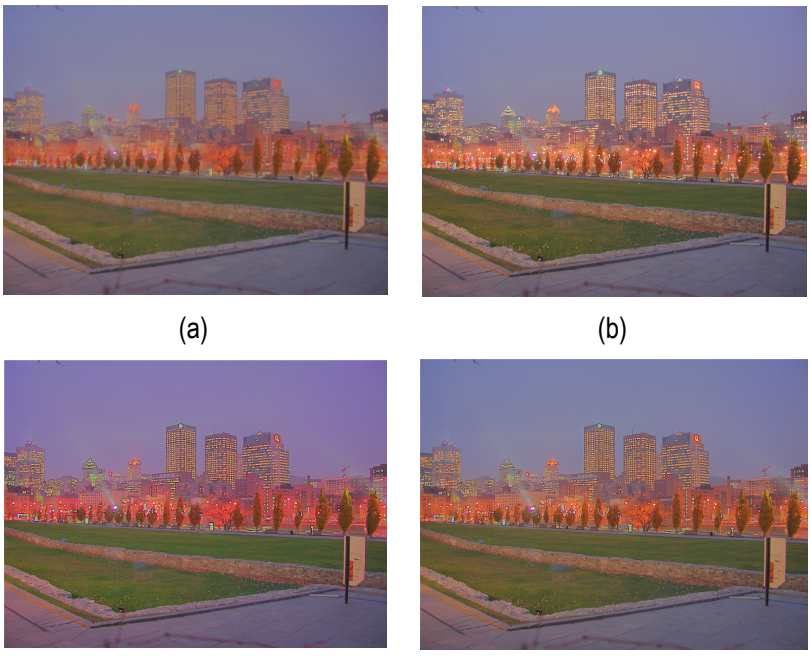

(a) (b)

(c) (d)

Figure 16: Tone mapped WDR image [24] using a. Gaussian filter (7x7), b. Median filter (7x7), c. Anisotropic Gaussian filter (7x7), d. Sigma filter (7x7).

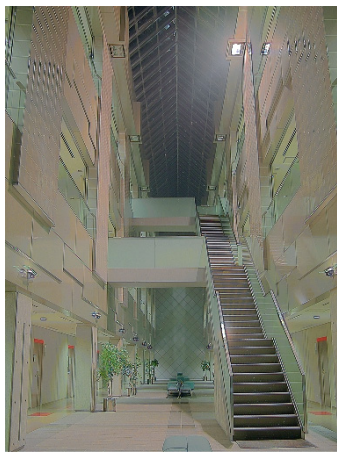

(a)

(b)

(c)

(d)

(e)

Figure 17: a. Gaussian filter (7x7), b. Median Filter (7x7), c. Bilateral Filter, d. Anisotropic Gaussian filter (7x7), e. Sigma Filter (7x7)

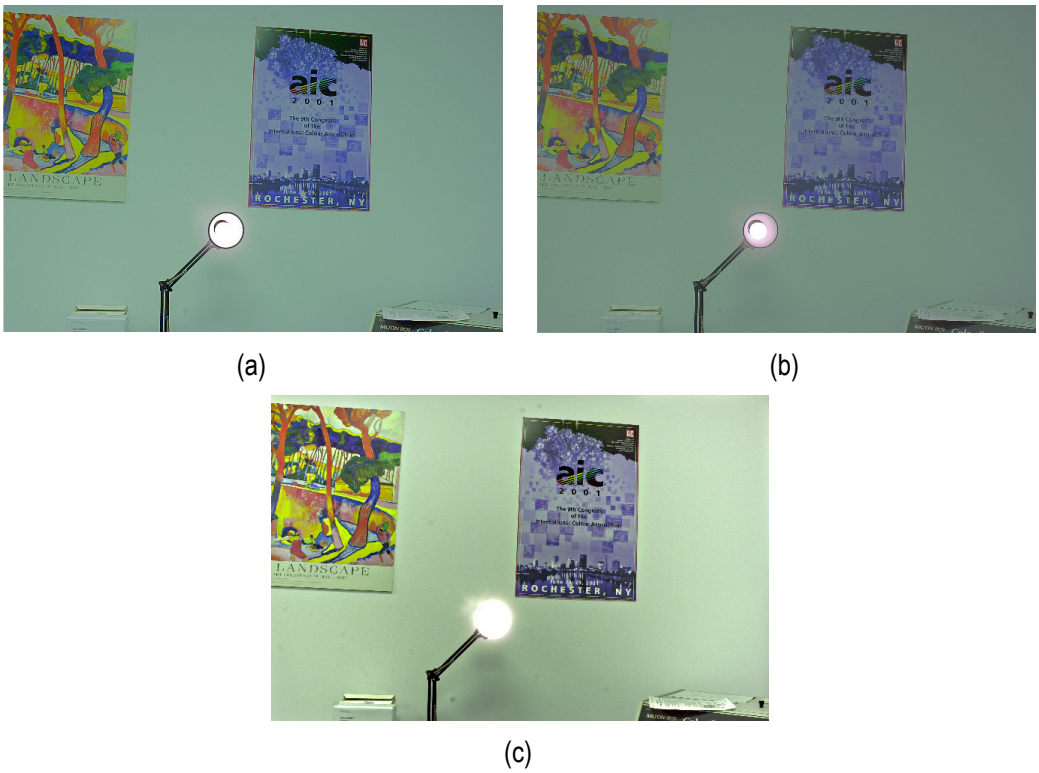

(a) (b)

(c)

Figure 18: Wall Image [19] using a. Meylan et al [5], b. Glozman et al [4] with Sigma filter, c. iCAM06 [8].

Results

The algorithm was implemented on MATLAB for both colored and monochrome. For colored images, demo as icing after tone mapping was performed using a simple bilinear interpolation. The colored images shown in Figure 19 show the MATLAB implementation using Gaussian filter.

Image Quality Assessment

Unlike other image processing techniques such as demosaicing, there is no ideal tone-mapped image that can be used to compare in an image quality assessment. Hence, having an objective image assessment will be difficult. In order to compensate for that, a subjective assessment was performed using 4 other available tone mapping operators [5, 6, 9, 26].

For this test, images were obtained from the Devebec library and other online sources [11, 25]. The test was aimed at checking how well the exponent-based tone mapper produced naturally good images (Figure 20). Tone mapping operators by Mantiuk et al, Fattal et al and Drago respectively [6, 9, 26], were obtained using the Windows application Luminance HDR that can be easily downloaded online [27].

The subjective study was broken into 2 separate tests that had the same image scenes except the tone mapping algorithms were different. Test 1 was done by 21 while test 2 was done by 31 people. The participants were not told which tone mapping operator was used to produce each image. For each question, the participants were asked to choose which image was the best in terms of naturalness and pleasantness. The images were randomly

arranged and the information of which tone mapping operator was used was hidden from the participants. The results are depicted in Tables 1 and 2.

After that the tone mapping operators were ranked based on the total number of votes obtained for each test. In Table 1, it can be seen that the exponent-based tone mapping algorithm [4] and Mantiuk et al's [26] algorithm had majority of the votes with the highest number of votes being for the exponent tone mapper. As can be seen in Table 2, the exponent-based algorithm by Glozman et al [4] and Meylan et al [5] were found to be amongst the best for majority of the images. It should be noted that both algorithms did not have any pre/post-processing such as histogram clipping done on the tone-mapped images produced.

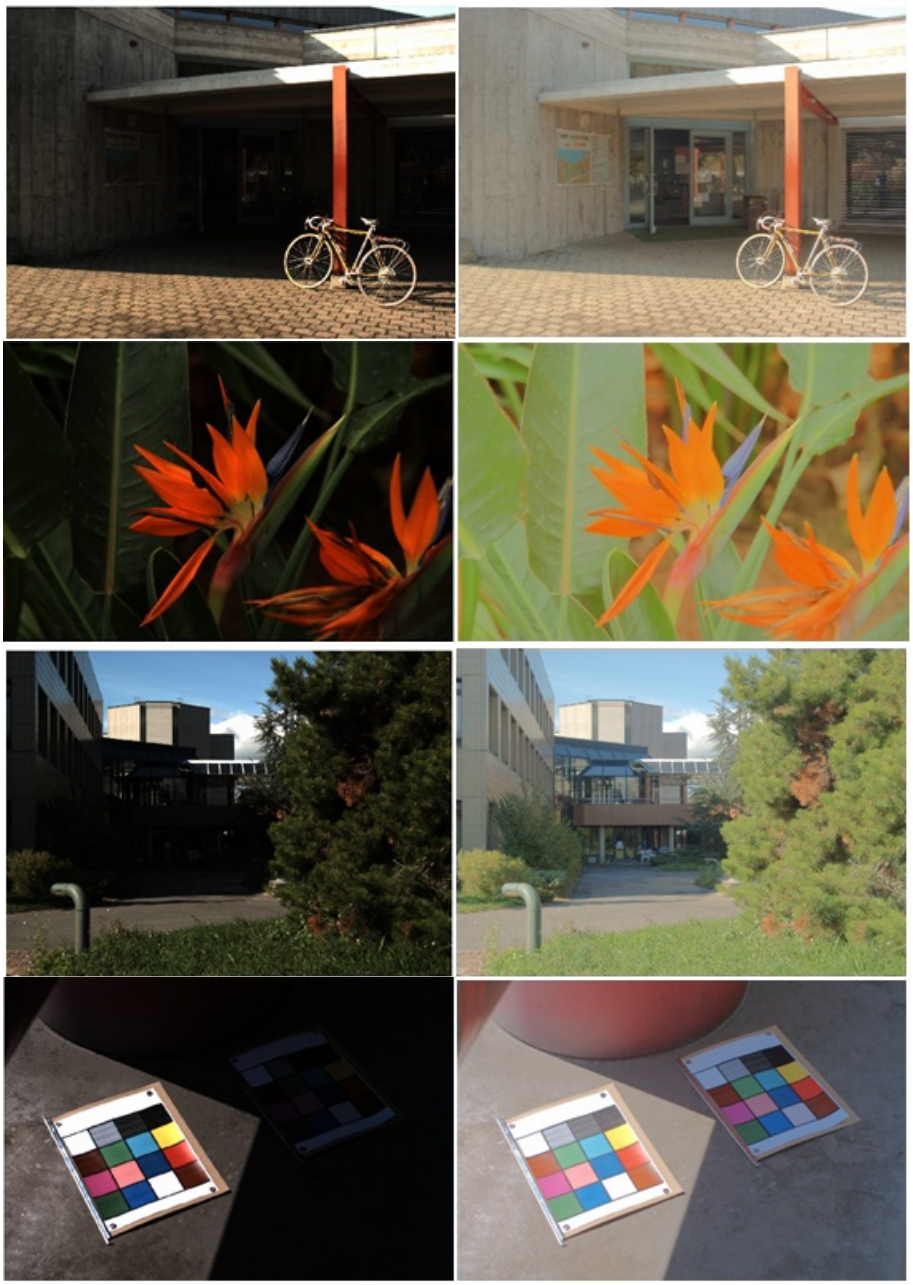

Figure 19: Tone mapped Images [25] Linear mapping (left) and Proposed automatic tuning (right).

Figure 20: Test images used in the subjective study. (Left to right): Auto, Lizard, Chapel (RAW), Synagogue

Table 1: Subjective Test results from Test 1

WDR Image	Glozman et al [4]	Drago et al [6]	Mantiuk et al [26]
Auto Image	11	2	8
Lizard	9	6	6
Chapel	5	2	14
synagogue	13	5	3
Total Votes	38	15	31

Table 2: Subjective Test Results from Test 2

WDR Image	Glozman et al [4]	Meylan et al [5]	Fattal el al [9]
Auto Image	8	15	8
Lizard	4	16	11
Chapel	18	6	7
synagogue	20	5	6
Total Votes	50	42	32

Conclusion

In this report, an in-depth analysis of an exponent-based tone mapping operator was performed. The relationships of the different components of the operators were explained. In addition, various experiments were made in order to descript the effects of various image filter needed for local adaptation processing. Median and sigma filters were found to be the best among the cases evaluated. However, the median filter resulted in loss of fine details in some tone mapped images which could be reduced by changing the kernel size. This tone mapping operator investigated will be useful for system-on-chip applications due to its simplicity.

Bibliography

[1] O. Yadid-Pecht and R. Etienne-Cummings, CMOS imagers: from phototransduction to image processing.: Springer, 2004.

[2] O. Yadid-Pecht and M. Herscovitz, "A Modified Multiscale Retinex Algorithm with an Improved Global Impression of Brightness for Wide Dynamic Range Pictures," Machine Vision and Applications, pp. 1-2, 2004.

[3] A. Belenky, A. Fish, O. Yadid-Pecht A. Spivak, "Wide Dynamic-Range CMOS Image Sensors -Comparative Performance Analysis," IEEE Trans. on Electron Devices, vol. 56, no. 11, pp. 2446-2461, November 2009.

[4] S. Glozman, T. Kats, and O. Yadid-Pecht, "Exponent Operator Based Tone Mapping Algorithm for Color Wide Dynamic Range Images," 2011.

[5] L. Meylan, D. Alleysson, and S. Susstrunk, "A Model of Retinal Local Adaptation for the Tone Mapping of Color Filter Array Images," The Journal of the Optical Society of America A, vol. 24, pp. 2807-2816, 2007.

[6] K. Myszkowski, T.Annen and N.Chiba, F.Drago, "Adaptive Logarithmic Mapping For Displaying High Contrast Scenes," EUROGRAPHICS, vol. 22, no. 2, pp. 419-426, 2003.

[7] T. Kats, S. Glozman, and O. Yadid-Pecht, "Efficient Color Filter Array luminance LOG based algorithm for Wide Dynamic Range (WDR) images compression," [Submitted].

[8] J. Kuang, Johnson G., and M. Fairchild, "iCAM06: A refined image appearance model for HDR image rendering," Journal of Visual Communication and Image Representation, vol. 18, no. 5, pp. 406-414, 2007.

[9] D. Lischinski and M. Werman R. Fattal, "Gradient domain high dynamic range compression," ACM Transactions on Graphics, vol. 21, no. 3, pp. 249-256, 2002.

[10] M. Stark, P. Shirley, and J. Ferwerda E. Reinhard, "Photographic tone reproduction for digital images," ACM Transactions on Graphics, vol. 21, no. 3, pp. 267-276, 2002.

[11] E. Reinhard, G. Ward, S. Pattanaik, and P. Debevec, High Dynamic Range Imaging: Acquisition, Display, and Image-Based Lighting.: Morgan Kurfmann Publishers, 2005.

[12] H. Shin, T. Yu, Y.r Ismail, and B. Saeed, "Rendering high dynamic range images by using integrated global and local processing," Optical Engineering, vol. 50, no. 11, p. 117002.

[13] D. Tamburrino, D. Alleysson, and L., Susstrunk, S. Meylan, "Digital camera workflow for high dynamic images using a model of retinal processing," IS&T/SPIE Electronic Imaging: Digital Photography IV, vol. 6817, January 2008.

[14] K. Jiangtao, Y. Hiroshi, L. Changmeng, M. Garrett, and M. Fairchild, "Evaluating HDR Rendering Algorithms," ACM Transactions on Applied Perception, vol. 4, no. 2, 2007.

[15] L. Meylan and S. Süsstrunk, "High dynamic range image rendering with a retinex-based adaptive filter," IEEE Transactions on Image Processing, vol. 15, no. 9, pp. 2820--2830, 2006.

[16] L. O'Gorman, M. Sammon, and M. Seul, Practical algorithms for image analysis: description, examples, programs, and projects.: Cambridge University Press, 2008.

[17] K. Myszkowski F. Drago. (2011, June) Aizu University's Atrium High Dynamic Range Source Images. [Online]. http://www.mpi-inf.mpg.de/resources/atrium/atriumHdr/index.html

[18] R. Gonzalez and R. Woods, Digital Image Processing, 3rd ed.: Prentice Hall, 2008.

[19] (2011, July) RIT MCSL High Dynamic Range Image Database. [Online]. http://www.cis.rit.edu/mcsl/node/557

[20] I. Pitas, Digital image processing algorithms and applications.: Wiley-IEEE, 2000.

[21] J. Lee, "Digital image smoothing and the sigma filter," Computer Vision, Graphics, and Image Processing, vol. 24, no. 2, pp. 255-269, 1983.

[22] A. Choudhury and G. Medioni, "Perceptually motivated automatic color contrast enhancement," in Computer Vision Workshops (ICCV Workshops), 2009 IEEE 12th International Conference, 2009, pp. 1893-1900.

[23] F. Durand and J. Dorsey, "Fast bilateral filtering for the display of high-dynamic-range images," ACM Transactions on Graphics, vol. 21, no. 3, pp. 257-266, 2002.

[24] G. Ward. High Dynamic Range Image Examples. [Online]. http://www.anyhere.com/gward/hdrenc/pages/originals.html

[25] L. Meylan and S. Süsstrunk, "Color image enhancement using a Retinex-based adaptive filter," in Proc. IS&T Second European Conference on Color in Graphics, Image, and Vision , 2004, pp. Vol. 2, pp. 359-363.

[26] R. Mantiuk and S. Daly and L. Kerofsky, "Display adaptive tone mapping," ACM Transactions on Graphics, vol. 27, no. 3, 2008.

[27] (2011, November) Luminance HDR. [Online]. http://qtpfsgui.sourceforge.net/

Authors' Information

C. Ofili is with the Department of Electrical and Computer Engineering, University of Calgary, Calgary, AB T2N 1N4, Canada.

S. Glozman is with the Department of Electrical and Computer Engineering, Ben-Gurion University of the Negev, Beer-Shev, Israel.

O. Yadid-Pecht is with the Department of Electrical and Computer Engineering, University of Calgary, Calgary, AB T2N 1N4, Canada.